Molecular Electrostatic Potentials from Crystal Diffraction: The Neurotransmitter γ-Aminobutyric Acid

R. F. Stewart* and B. M. Craven‡

*Department of Chemistry, Carnegie Mellon University, Pittsburgh, PA 15213, and ‡Department of Crystallography, University of Pittsburgh, Pittsburgh, PA 15260 USA

ABSTRACT Given the electronic charge parameters obtained from a diffraction study of the charge density distribution in a crystal, a mathematical procedure is presented for deriving the electrostatic potential. The procedure allows the mapping of electrostatic potential for a molecule or group of molecules removed from the crystal structure but with each molecule retaining the effects of polarization owing to the original crystal environment. The method is applied for the neurotransmitter γ-aminobutyric acid. The potential for a γ-aminobutyric acid molecule is analyzed in terms of a simple model that is suitable for rapid computations concerned with Coulombic molecular interactions. Outside the molecular envelope at 1.2 Å from the atomic nuclei, the total potential is well represented by a sum of spherical atom contributions with $V(r) = (q/r) + \exp(-\beta r^2)$. The most important aspherical component in the potential is the dipole contribution from the hydrogen atoms. This can be represented as $V(r, \phi) = (0.162 \cos \phi)/(r^2 + 0.615)$. Here, V is in e/Å, r is the distance from each nucleus in Å, q is the experimentally determined net atomic charge in electron units, and ϕ is the angle between r and the bond X—H. We obtain β = 1.47, 1.66, 1.83 Å^{-2} for C, N, and O respectively. For H, no term in β is needed.

INTRODUCTION

Most studies of electron density distributions in crystals are now carried out using a pseudoatom model (Hirshfeld, 1971; Stewart, 1976) to represent the charge distribution around each atom center. In this way, the total charge distribution in the unit cell is described in terms of atomic positional, thermal vibrational, and electronic charge parameters. These parameters are then fitted by least squares to x-ray or neutron diffraction data. In principle, the pseudoatom model allows the deconvolution of the charge distribution from the atomic thermal displacements in the crystal and leads to the mapping of the charge density distribution for a stationary array of pseudoatoms. It is also possible to map other electrostatic properties derived from the experimental charge parameters. Among such properties, the electrostatic potential is receiving increased attention. Experimental electrostatic potentials can be mapped either within the crystal unit cell (Stewart, 1979) or for a molecule or group of molecules removed from the crystal (Stewart, 1982; Stewart, 1991).

Maps of the electrostatic potential for a molecule removed from the crystal explicitly show regions of electronegativity and electropositivity that are not easily inferred from inspection of the parent charge density distribution. From a potential map, energetically favorable coulombic interactions of a molecule with its neighbors can readily be understood, since these will involve the overlap of electropositive with electronegative regions, to give at least a partial cancellation. The way in which this comes about has been demonstrated for hydrogen-bonded molecular clusters of phosphorylethanolamine (Swaminathan and Craven, 1984) and urea (Stewart, 1991). A significant aspect of the potential when determined experimentally is that after removal from the crystal the molecule retains the effects of polarization by its original crystal environment.

The recent redetermination of the crystal structure of ammonium dimethylphosphate (Klooster and Craven, 1992) included a detailed study of the molecular electrostatic potential. The two phosphodiester O atoms were found to be considerably less electronegative than the two phosphoryl O atoms. The two phosphoryl O atoms, which are chemically equivalent because of the twofold symmetry in an isolated dimethylphosphate anion, were found to have significantly different electronegativities in the anion removed from the crystal. In the crystal, the twofold symmetry is closely preserved. The difference in the phosphoryl O atoms is attributed to the polarizing effect of the hydrogen bonding in the crystal. Thus the more electronegative phosphoryl O atom forms three N—H ··· O hydrogen bonds, whereas the other O atom forms only one. This simple crystal structure provides an indication of the polarization effects to be expected for the phosphodiester groups in more complicated biological systems.

Our present aim is threefold. First, we describe a general mathematical procedure whereby the charge parameters of the pseudoatom model can be used to map the electrostatic potential. This procedure has not previously been described in detail, although it was first outlined by Stewart (1979, 1982) and has been used since then to map the electrostatic potential for imidazole and 9-methyladenine (Stewart, 1982), phosphorylethanolamine (Swaminathan and Craven, 1984), the complex of thiourea with parabanic acid (Weber and Craven, 1987), parabanic acid (He et al, 1988), 1-methyluracil (Klooster et al., 1992), urea, and benzene (Stewart, 1991). A similar procedure has been described by Su and Coppens (1992) and used to obtain a map of electrostatic potential for benzene that is very similar to that of Stewart (1991). Both maps were derived using diffraction

Received for publication 11 February 1993 and in final form 7 May 1993.

Address reprint requests to Dr. Bryan M. Craven.

0006-3495/93/09/998/08 $2.00

data for benzene collected by Jeffrey et al. (Department of Crystallography, University of Pittsburgh, Pittsburgh, PA, personal communication, 1991).

Second, we present, as a further application of the Stewart procedure, maps of the electrostatic potential for γ-aminobutyric acid (GABA). The electrostatic properties of GABA are of interest because this is a highly polar molecule that functions as the main inhibitory neurotransmitter in the mammalian central nervous system (Hösli and Hösli, 1983; De Robertis, 1986). The charge parameters for GABA were obtained from new least-squares refinements based on the neutron diffraction data of Weber et al. (1983) and the x-ray data of Craven and Weber (1983).

Third, we analyze the experimental potential for GABA in terms of a simple model intended to be useful for rapid computations involving Coulombic interactions of molecules containing C, N, O, and H atoms.

METHOD

We describe a procedure to evaluate the total electrostatic potential given the charge distribution for an assembly of pseudoatoms. Such an assembly might constitute a molecule or group of molecules taken from a crystal structure.

The potential $\phi(\vec{r})$ at $\vec{r}$ (Fig. 1) due to a total charge density distribution, $\rho(\vec{r})$, is

$$\phi(r) = \int \rho(\vec{r}')|\vec{r} - \vec{r}|^{-1}\, d^3\vec{r}'. \tag{1}$$

Note that $\rho(\vec{r}')$ is convoluted into $|\vec{r} - \vec{r}|^{-1}$. It is convenient to carry out a Fourier transformation so as to recast Eq. 1 as an integration in reciprocal or $\vec{K}$ space. With the identity

$$|\vec{r} - \vec{r}|^{-1} = (2\pi^2)^{-1} \int e^{-i\vec{K}\cdot(\vec{r}-\vec{r}')}|\vec{K}|^{-2}\, d^3\vec{K};$$

$$i = \sqrt{-1}, \tag{2}$$

Eq. 1 can be written

$$\phi(\vec{r}) = (2\pi^2)^{-1} \int F(\vec{K}) e^{-i\vec{K}\vec{r}} |\vec{K}|^{-2}\, d^3\vec{K} \tag{3}$$

in which $F(\vec{K})$ is the form factor of $\rho(\vec{r}')$,

$$F(\vec{K}) = \int \rho(\vec{r}') e^{i\vec{K}\vec{r}}\, d^3\vec{r}'. \tag{4}$$

If $\rho(\vec{r}')$ is a superposition of pseudoatoms (with the nuclei included) that are located at $\vec{R}_P$, then

$$F(\vec{K}) = \sum_P \left[Z_P - \sum_{lm\pm} C_{P,lm\pm} i^l f_{P,l}(K) Y_{lm\pm}(\Omega_{\vec{K}}) \right] e^{i\vec{K}\vec{R}_P} \tag{5}$$

In Eq. 5 Z_P is the nuclear charge of pseudoatom P, the $Y_{lm\pm}$ are surface harmonics (+ for cos $m\phi_{\vec{K}}$ and − for sin $m\phi_{\vec{K}}$) in the angular components of $\vec{K}(\Omega_{\vec{K}})$, and the $C_{P,lm\pm}$ are electron population coefficients, extracted from x-ray structure factors. The $f_{P,l}(K)$ is the Fourier-Bessel transform of a pseudoatom radial electron distribution function:

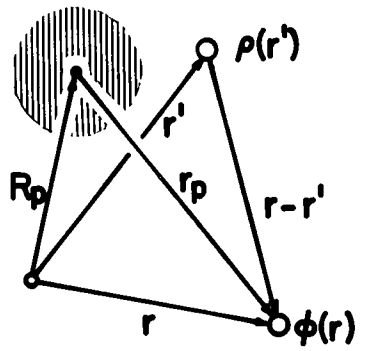

FIGURE 1 Contribution of the pseudoatom at $\vec{R}_P$ to the electrostatic potential $\phi(\vec{r})$.

$$f_{P,l}(K) = \int_0^\infty \rho_{P,l}(\alpha, r') j_l(Kr') r'^2\, dr' \tag{6}$$

Note that Eq. 5 describes a superposition of stationary pseudoatoms. The atomic thermal vibrational functions, such as $\exp(-\frac{1}{2}\vec{K}^t U_P \vec{K})$, which occur as an additional factor in the crystallographic form factor, here have been set to unity. With Eq. 5, we can treat Eq. 3 as a sum over individual pseudoatom electrostatic potentials, $\phi_P(\vec{r}_P)$ (with $\vec{r}_P = \vec{r} - \vec{R}_P$). Thus we focus on

$$\phi_P(\vec{r} - \vec{R}_P) = (2\pi^2)^{-1} \tag{7}$$

$$\times \int \left[Z_P - \sum_{lm\pm} C_{P,lm\pm} i^l f_{P,l}(K) Y_{lm\pm}(\Omega_{\vec{K}}) \right] e^{-i\vec{K}(\vec{r} - \vec{R}_P)}\, dK\, d\Omega_{\vec{K}}$$

Integration over $d\Omega_{\vec{K}}$ generates surface harmonics in the angular components of $\vec{r} - \vec{R}_P = \vec{r}_P$:

$$\phi_P(r_P) = \frac{Z_P}{|\vec{r} - \vec{R}_P|} - \sum_{lm\pm} C_{P,lm\pm} \left[\frac{2}{\pi} \int_0^\infty f_{P,l}(K) j_l(Kr_P)\, dK \right] Y_{lm\pm}(\Omega\vec{r}_P). \tag{8}$$

In going from Eq. 7 to Eq. 8, note that $\int_0^\infty j_0(kx)\, dk = \pi/2x$. To develop the function of r_P in Eq. 8 further, we make use of the identity

$$j_l(x) = (2l + 1)^{-1} x[j_{l+1}(x) + j_{l-1}(x)]. \tag{9}$$

With Eq. 9 in Eq. 8, and considering only the expression in square brackets,

$$g(r_P) = \frac{2}{\pi} \int_0^\infty f_{P,l}(K) j_l(Kr_P)\, dK = (2l + 1)^{-1} r_P \left[\frac{2}{\pi} \int_0^\infty f_{P,l}(K) \{ j_{l+1}(Kr_P) + j_{l-1}(Kr_P) \} K\, dK \right]. \tag{10}$$

When the radial form factor in Eq. 6 is substituted into Eq. 10,

$$g(r_P) = (2l + 1)^{-1}\left(\frac{2}{\pi}\right)r_P \times \left\{ \int_0^\infty \rho_{P,l}(r)\left[\int_0^\infty j_{l+1}(Kr_P)j_l(Kr)K\,dK + \int_0^\infty j_l(Kr)j_{l-1}(Kr_P)K\,dK \right] r^2\,dr \right\}. \quad (11)$$

The integrals in the square brackets in Eq. 11 are the discontinuous integrals of Weber-Schafheitlin (Watson, 1966),

$$\left(\frac{2}{\pi}\right)\int_0^\infty j_{l+1}(xt)j_l(yt)t\,dt = \begin{cases} y^l/x^{l+2}, & 0 < y < x \\ 1/2x^2, & 0 < y = x. \\ 0, & y > x > 0 \end{cases} \quad (12)$$

With Eq. 12, we see that Eq. 11 reduces to the result

$$g(r_P) = (2l + 1)^{-1}\left[r_P^{-(l+1)} \int_0^{r_P} \rho_{P,l}(r)r^{l+2}\,dr + r_P^l \int_{r_P}^\infty \rho_{P,l}(r)r^{1-l}\,dr \right]. \quad (13)$$

Thus the contribution of the Pth pseudoatom to the total potential at r_P (8) is obtained as the sum of three parts: the contribution of the nucleus, the electron density in the shell extending from the nucleus and having radius r_P, and the electron density in the shell from radius r_P to infinite distance. From Eq. 13 it can be seen that the pseudoatom potential decreases with increased distance from the nucleus in proportion to $r_P^{-(l+1)}$, which corresponds to $1/r_P$ for the monopole contribution, $1/r_P^2$ for the dipoles, $1/r_P^3$ for the quadrupoles, and $1/r_P^4$ for the octapoles. Therefore, with increasing distance from the nucleus, the higher multipole terms become relatively diminished in importance.

For computations as in the application to GABA (following section), we use Hartree-Fock atomic wave functions with Slater-type functions and with coefficients as tabulated by Clementi (1965). The spherical charge density for the Pth pseudoatom is then given by the sum of orbital products

$$\rho_P = \frac{1}{4\pi}\left\{ \sum_j D_j r^{n_j}\exp(-\alpha_j r) + (p_v)_P \sum_k D_k \kappa_P^{n_k+3} r^{n_k}\exp(-\alpha_k \kappa_P r) \right\}. \quad (14)$$

Here, the first summation contains terms for the invariant inner shells (K shells with two electrons for C, N, and O). The second summation contains terms for the valence shell. The coefficients D_k are normalized to give a one-electron radial density function, and the parameter $(p_v)_P$ is the valence shell electron population parameter ($C_{P,00}$), which is fitted by least squares to the diffraction data. For the valence shell, we introduce as an additional variable the radial contraction parameter κ_P, which is also fitted to the diffraction data. Equation 14 represents the pseudoatom model described by Coppens et al. (1979).

Higher multipole terms have the form

$$\rho_P(r, \theta, \phi) = \frac{1}{4\pi} C_{P,lm\pm} r^n \exp(-\alpha_P r) Y_{lm\pm}(\theta, \phi)$$

where $C_{P,lm\pm}$ is the electron population parameter and α_P is a radial exponent that is often assumed to have a standard value (Hehre et al., 1969).

The integrations in Eqs. 8 and 13 can then be reduced by standard procedures to give

$$\phi_P(\vec{r}_P) = \frac{Z}{|\vec{r}_P|} - \sum_j D_j \left\{ \frac{A_{n_j+2}(\alpha_j, |\vec{r}_P|)}{|\vec{r}_P|} + B_{n_j+1}(\alpha_j, |\vec{r}_P|) \right\} - (p_v)_P \sum_k D_k \left\{ \frac{A_{n_k+2}(\alpha_k, \kappa_P|\vec{r}_P|)}{|\vec{r}_P|} + \kappa_P B_{n_k+1}(\alpha_k, \kappa_P|\vec{r}_P|) \right\}, \quad (15)$$

together with similar terms from the higher multipoles. The latter contain $Y_{lm\pm}(\theta, \phi)$ as an additional factor.

In Eq. 15, we define

$$A_n(\alpha, x) = \int_0^x r^n \exp(-\alpha r)\,dr = \left(\frac{n!}{\alpha^{n+1}}\right)[1 - \exp(-\alpha x)E_n(\alpha x)]$$

and

$$B_n(\alpha, x) = \int_x^\infty r^n \exp(-\alpha r)\,dr = \left(\frac{n!}{\alpha^{n+1}}\right)\exp(-\alpha x)E_n(\alpha x)$$

with

$$E_n(\alpha x) = 1 + \alpha x + \frac{(\alpha x)^2}{2!} + \cdots + \frac{(\alpha x)^n}{n!}.$$

Computer programs for these calculations have been incorporated as part of the VALRAY (Stewart and Spackman, 1983) and POP packages (Craven et al., 1993) and are available from the respective authors. The VALRAY program is more flexible in several respects; for example, Laguerre-type radial functions may be used (van der Wal and Stewart, 1984). The GABA refinements and mapping of electrostatic potentials were carried out with the POP system.

EXPERIMENTAL PROCEDURES

An experimental charge density study of GABA based on x-ray data collected at 122 K was reported by Craven and Weber (1983; henceforth CW),

but this did not include a mapping of the molecular electrostatic potential. CW assumed a pseudoatom model involving invariant Hartree-Fock neutral spherical atomic cores. The deformation charge density consisted of terms from a complete multipole expansion from monopole through octapole, each term having a single Slater-type radial function. Fixed nuclear positional parameters for all atoms were taken from Weber et al. (1983; henceforth WCM), who reported a neutron diffraction study carried out at the same temperature. Fixed anisotropic thermal parameters for H atoms were also taken from WCM, but for the heavier atoms CW refined the anisotropic thermal parameters using their own x-ray data. This was because the resulting values were systematically different from the corresponding WCM neutron diffraction values.

We have carried out new refinements using the CW x-ray data. These consist of 3394 reflections $|F| > 4\sigma$ extending to $\sin\theta/\lambda = 1.30$ Å^{-1} (MoKα radiation). We adopted a different pseudoatom model from the earlier study. For C, N, and O, we assumed the more flexible model given by Eq. 14 above. Hartree-Fock atoms were assumed with invariant K-shell cores populated by two electrons. The Hartree-Fock spherical valence shell was assigned a variable population parameter (p_v) for each atom and a variable radial expansion parameter (κ) having the same value for the four C atoms (κ_c) and the two O atoms (κ_o). For the deformation terms a complete multipole expansion (dipole to octapole) was assumed, each multipole term having a single Slater-type radial function with a standard value for the exponent (6.42, 7.37, and 8.5 Å^{-1} for C, N, and O, respectively; Hehre et al., 1969). For H atoms, the multipole expansion involved monopole through quadrupole terms with a fixed standard radial exponent, 4.54 Å^{-1}.

Using this model, very good agreement was obtained with the neutron thermal parameter values U^{ij} reported by WCM.[1] Consequently, all nuclear positional and thermal parameters were assigned fixed WCM values, and only the 196 charge parameters were variables in the least squares refinement.

Full-matrix least-squares minimization of the residual $\Sigma w\Delta^2$ with $\Delta = |F_{obs}| - |F_{cal}|$ gave final values $R_w(F) = 0.044$, $R(F) = 0.054$, and goodness of fit = 1.635.[2] In the refinement, the number of electrons in the molecule was unconstrained. Whereas ideal values would be 14 K-shell electrons and 42 valence electrons, the observed relative values after scaling give 14.11(2) and 41.89(13) electrons, respectively. In Table 1, values of the pseudoatom valence shell charges are scaled to give $\Sigma p_v = 42$. The electrostatic potential derived from this refinement is shown in Fig. 2 (*a*, *b*, and *c*).

A second refinement was carried out in which all pseudoatoms were assumed to be spherically symmetric. Neglecting the higher multipoles, the number of charge parameters was reduced to the 16 values for p_v and the three values for κ, so that with the inclusion of an overall scale factor, the total number of variables was 20. This refinement gave final values $R_w(F) = 0.058$, $R(F) = 0.065$, and goodness of fit 2.096. The relative charges obtained were 13.59(2) K-shell and 42.41(17) valence shell electrons per molecule. The scaled valence shell charges from this refinement are also shown in Table 1. The electrostatic potential derived from the spherical atom refinement is mapped in Fig. 2 *d*.

TABLE 1 Atomic charge parameters for GABA

Atom	(a)	(b)	(c)
N	5.52 (9)	5.29 (7)	1.04
C1	3.91 (6)	3.90 (6)	1.00
C2	4.09 (6)	4.05 (6)	1.01
C3	3.87 (6)	3.91 (6)	0.99
C4	3.93 (5)	3.65 (6)	1.07
O1	6.34 (5)	6.30 (5)	1.01
O2	6.46 (5)	6.36 (5)	1.02
H1	0.74 (3)	0.79 (3)	0.94
H2	0.72 (4)	0.81 (3)	0.89
H3	0.69 (4)	0.84 (3)	0.82
H4	0.97 (4)	1.00 (3)	0.97
H5	0.92 (4)	1.02 (3)	0.90
H6	0.90 (3)	0.97 (3)	0.93
H7	0.94 (4)	0.99 (3)	0.95
H8	1.00 (4)	1.04 (3)	0.96
H9	1.00 (4)	1.10 (3)	0.91
	κ-values		
N	0.979 (8)	1.003 (8)	0.98
C	1.015 (6)	1.048 (6)	0.97
O	0.974 (4)	0.968 (4)	1.01
H	1.0	1.0	(Fixed)

(a): Number of valence shell electrons (p_v) obtained in the refinement with the pseudoatom model including higher multipoles. A table including electron population parameters for the higher multipole terms is available from the authors.
(b): Corresponding values obtained for the spherical atom refinement.
(c): The ratio (a):(b).

RESULTS AND DISCUSSION

The electrostatic potential for GABA

The zwitterionic character of GABA is well illustrated in the maps of the experimentally determined total electrostatic potential for a molecule removed from the crystal (Fig. 2). For each pseudoatom, the potential has an infinite positive value at the nucleus. We map only the regions with $V(r) < 0.5e$/Å.

It can be seen that there is an extensive region of electropositivity around the ammonium group and an electronegative region around the carboxylate group. The electronegativity is developed more extensively around atom O(2) than O(1). In the crystal structure, O(2) forms two N—H · · · O hydrogen bonds, whereas O(1) forms only one. To some extent, the enhanced electronegativity at O(2) may be a crystal polarization effect similar to that reported by Klooster and Craven (1992). However, in GABA, differences at the carboxylate oxygen atoms are expected because these atoms have different intramolecular environments. It is of interest to compare the electrostatic potential around O(2) in Fig. 2 *a* with the deformation charge density as shown by CW in their figure 4. CW show lobes of nonbonded deformation density closely directed along the O(2) · · · H hydrogen bonds. It might be inferred that the loan pair density has a directional effect on the hydrogen bonding, but this would not be justified because the electrostatic potential around O(2) is broad and almost featureless.

CW observed that the net atomic charge at H(6) in GABA was intermediate between those of the N—H and the other C—H hydrogen atoms. They noted that the electropositivity of H(6) might be correlated with the short intramolecular distances N · · · H(6) and H(6) · · · O(1) of 2.64 and 2.54 Å, respectively, and postulated an intramolecular bridge N · · · H · · · O stabilizing the folded molecular conformation. After our new refinements, H(6) is no more electropositive than other C—H hydrogen atoms (Table 1). Owing to the proximity of the electronegative O(1) and N atoms, the electropositive region around H(6) (Fig. 3) is contracted when compared with the other C—H hydrogen atoms. However, we cannot say that H(6) is more polarized because of a bridging interaction.

[1] CW reported small but significant atomic anharmonic vibrations which were most notable for O(1). The third-order anharmonic thermal parameters determined by CW from their X-ray data were used as fixed values in all the refinements described here.

[2] $R(F) = \Sigma|\Delta|/\Sigma|F_{obs}|$; $R_w(F) = \{\Sigma w\Delta^2/\Sigma w|F_{obs}|\}^{1/2}$ and the goodness of fit is $\{\Sigma w\Delta^2/(m-n)\}^{1/2}$.

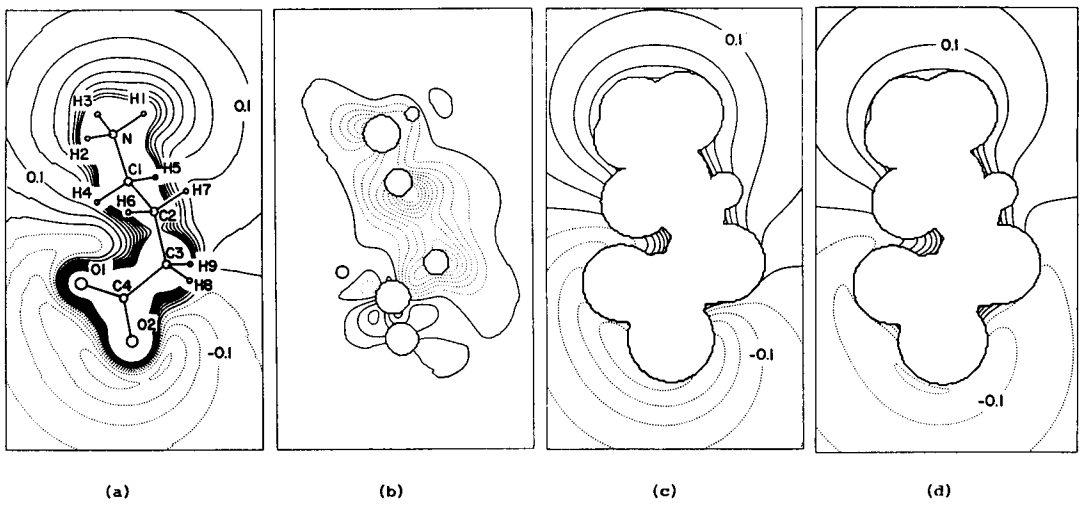

FIGURE 2 Experimental electrostatic potential for GABA in the plane through the molecular center of mass and normal to the axis of maximum inertia. This is the section $y = 0$ with the atomic coordinates as given in Table 2. Contours are at intervals 0.05 e/Å up to 0.50 e/Å with contours dotted in the regions of electronegativity. Maps are for an area 7 Å × 12 Å. (*a*) Map derived from the X-ray refinement with the full pseudoatom model including higher multipoles. (*b*) Map as in (*a*), but including only the contributions of pseudoatom dipoles, quadrupoles, and octapoles. Circles are the intersections of spheres 0.5 Å in radius with atomic nuclei as centers. (*c*) Map obtained assuming atomic contributions $V(r) = (q/r) + \exp(-\beta r^2)$. The potential is mapped outside the molecular envelope at 1.2 Å from the atomic nuclei. (*d*) Map derived from the X-ray refinement with spherical pseudoatoms, calculated as in (*c*).

TABLE 2 Atom coordinates (Å)

Atom	(*x*)	(*y*)	(*z*)
N	−0.397	−0.103	−2.973
C1	0.049	−0.562	−1.633
C2	0.701	0.572	−0.867
C3	1.070	0.170	0.558
C4	−0.120	0.025	1.502
O1	−1.247	0.402	1.129
O2	0.110	−0.476	2.641
H1	0.432	0.263	−3.519
H2	−1.118	0.637	−2.862
H3	−0.838	−0.895	−3.507
H4	−0.827	−0.928	−1.091
H5	0.749	−1.387	−1.779
H6	0.002	1.413	−0.843
H7	1.600	0.894	−1.411
H8	1.723	0.926	1.012
H9	1.641	−0.766	0.572

Coordinates are derived from the nuclear positional parameters (WCM) by a transformation to the (Cartesian) molecular inertial axes. The origin is at the molecular center of mass. The *y*-axis corresponds to the maximum moment of inertia (427 dalton·Å²) and is normal to the best plane with respect to the atomic nuclei. The *z*-axis corresponds to the minimum moment of inertia (81 dalton·Å²) and is the best line.

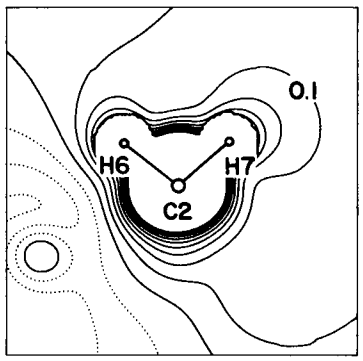

FIGURE 3 Experimental electrostatic potential in the plane of the H(6)--C(2)-H(7) methylene group, as derived from the pseudoatom model including higher multipoles. Contours are at intervals of 0.05 to 0.50 e/Å. The map is for an area of 3 Å × 3 Å. The electronegative region comes from the proximity of O(1). In this projection, N almost superposes on C(2).

A simplified model for the electrostatic potential

For molecular mechanics and molecular dynamics calculations, the Coulombic terms are an important component of the assumed force field. These terms are currently derived by theoretical or semiempirical procedures (Brooks et al., 1983; Weiner et al., 1986). It would be preferable to have a simple model based on experiment. A promising beginning has been made by Pearlman and Kim (1990), who obtained atomic charges from refinements of several nucleosides and nucleotides by using a simplified spherical atom version of the Coppens model (1979). Pearlman and Kim mapped electrostatic potentials for these molecules using their atomic charges as point charges. We now describe a similar approach, but we also include an assessment of the justifications and limitations when we apply a simple model for the potential.

As a first simplification, we note that for an atom with a given net charge q, the valence shell expansion parameter κ has very little effect on the electrostatic potential. In Fig. 4 *a* we show the radial potential for an isolated spherical Hartree-Fock oxygen atom with a valence charge $p_v = 6.4$ or net atomic charge $q = Z_v - p_v = 6.0 - 6.4 = -0.4$. When the valence shell density is expanded ($\kappa = 1.00$ to 0.96) there is very little change in the potential. The parameters used for Fig. 4 are similar to those obtained for GABA (Table 1). We emphasize that in the least-squares refinement based on the x-ray data, κ is an important variable that has a strong influence on the magnitude obtained for the valence charge, p_v.

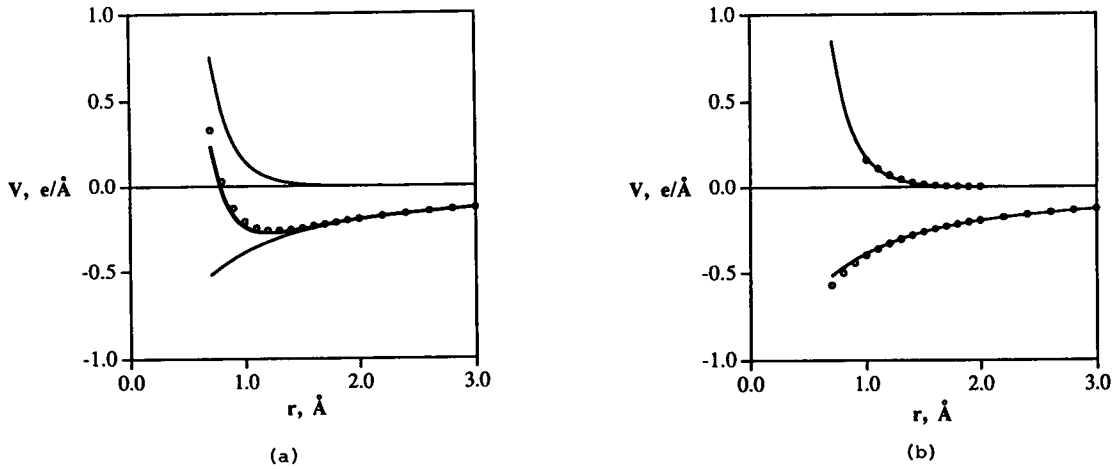

FIGURE 4 Radial potential functions for an isolated spherical Hartree-Fock oxygen atom with net charge $q = -0.4$. The top curve ($V \geq 0$) is for the neutral core (nucleus and 8 electrons). The bottom curve ($V < 0$) is from the valence shell, populated by 0.4 electrons. (*a*) Total radial potential for $\kappa = 1.00$ is shown as the bold line. Points superposed are the total potential when the valence shell is expanded ($\kappa = 0.96$). (*b*) Radial potentials for the expanded atom ($\kappa = 0.96$). Points superposed are for the functions $\exp(-1.83\ r^2)$ on the top curve and $-0.4/r$ for the bottom curve.

However, having obtained p_v, the potential is well represented, when κ is neglected.

More importantly, Fig. 4 *b* shows that for distances $r > 2$ Å, the contribution to the radial potential from the neutral Hartree-Fock core is effectively zero. The potential for the remaining spherical component of the valence shell density is accurately given by a simple point charge model with $V(r) = q/r$. For smaller r, we include a Gaussian function for representing the potential resulting from the neutral core. For carbon, nitrogen, and oxygen pseudoatoms, $V(r) = q/r + \exp(-\beta r^2)$ gives a fit within $0.003e$/Å when r is greater than the van der Waals radius. This expression gives V in e/Å units when r is in Å and q is a multiple of the electron charge. We obtain $\beta = 1.47$ Å^{-2} ($r > 1.2$ Å) for carbon, 1.66 Å^{-2} ($r > 1.3$ Å) for nitrogen, and 1.83 Å^{-2} ($r > 1.2$ Å) for oxygen. As an example, the quality of the fit for oxygen is shown in Fig. 4 *b*. For hydrogen, the nucleus shielded by one electron having a single Slater-type radial density function (exponent $\alpha = 4.54$ Å^{-1}) gives a potential that decreases to $0.002e$/Å at $r = 0.90$ Å. Therefore, for hydrogen we neglect the Gaussian term.

When the potential is computed, a major simplification is achieved if the contribution of the pseudoatom higher multipole terms can be neglected. We have noted above (Eq. 13) that these contributions become less important with increasing distance from the atomic nuclei. Indeed, from Fig. 2 *b* it can be seen that the higher multipole contribution to the total potential is negligible beyond about 2.5 Å from the atomic nuclei. In Fig. 2 *c* we map the electrostatic potential for GABA using our proposed simple expressions for the radial potential and neglecting all higher multipole contributions. Beyond the molecular envelope at 1.2 Å from the atomic nuclei, Fig. 2 *c* is almost indistinguishable from the corresponding map computed from the spherical component of the complete multipole potential (not shown). We point out that the potential obtained using our simplified expression (Fig. 2 *c*) is very similar to the total potential (Fig. 2 *a*), and furthermore, the calculations required only a tenth of the computing time.

The most important effect of the higher multipoles on the potential is likely to be the contribution from the hydrogen atom dipoles. The dipole charge deformation is very significant for hydrogen atoms because it describes how the electron density is enhanced in the X—H covalent bonding region (X = C, N, or O) and depleted on the other side of the proton. A survey of experimental charge density studies (Craven, 1987) indicates an average local atomic dipole moment $|\mu| = 0.94$ Debye for 25 different H atoms in C—H groups. There are few available examples for N—H and O—H groups, but the indications are that $|\mu|$ for these hydrogens is slightly smaller. Assuming an average dipole deformation, the hydrogen dipole potential is $0.05e$/Å at a distance of 1.7 Å from the proton. In the region $r > 1.0$ Å, we obtain a fit within $0.002e$/Å for the average hydrogen dipole potential using the expression $(0.162 \cos \phi)/(r^2 + 0.615)$, where ϕ is the angle between the directions of r and the X—H bond. When the hydrogen net charge is small, as in C—H groups, the dipole contribution can predominate for distances $r > 1.0$ Å from the proton. In Fig. 5, we map the potential in the plane of the methylene group at C(3) in which both hydrogens H(8) and H(9) happen to have zero net charge (Table 1). Thus the potential obtained neglecting the higher multipole contribution (Fig. 5 *b*) is effectively zero beyond 0.7 Å from the protons. The total potential (Fig. 5 *a*) is very similar to the potential obtained when the dipole contribution is included using our approximation (Fig. 5 *c*).

We conclude that at distances corresponding to the molecular van der Waals envelope and beyond, the total experimental electrostatic potential is given within a few parts per hundred by a spherical atom model using a simple expression with two terms. The most serious error will be

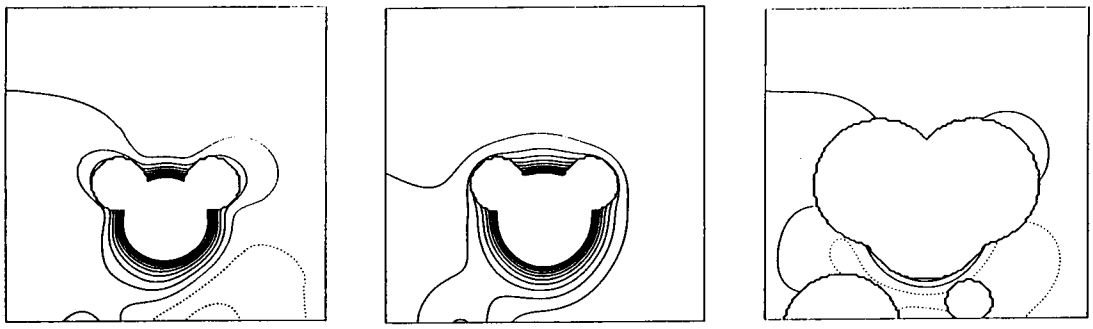

FIGURE 5 Electrostatic potential for a complete GABA molecule in the section through the methylene group, H(8)-C(3)-H(9). Atom H(8) is on the right. Contours are at intervals 0.05 e/Å, up to 0.50 e/Å. In (a) and (b), the hydrogen atoms are enclosed by circles of radius 0.5 Å. In (c), the atoms are enclosed by the envelope at 1.2 Å from all atom centers. Maps are of areas 3 Å × 3 Å. (a) Map derived from the X-ray refinement with the full pseudoatom model, including higher multipoles. (b) Map as in (a), but omitting the contributions of dipole, quadrupole, and octapole terms. For this methylene group, net atomic charges happen to be zero for both H(8) and H(9). (c) Map obtained assuming simplified expressions for the potential. Hydrogen atom dipole contributions are included as $V(r,\phi) = 0.165 \cos \phi/(r^2 + 0.615)$. This map shows portions of the molecular envelope around H(4) at bottom left and H(6) at bottom center.

introduced by neglecting the dipole contribution for the hydrogen atoms.

We emphasize that the simple expressions described above are intended to be used with atomic net charges derived from an x-ray refinement that includes the higher multipoles. For molecules with many atoms (>50), such full refinements involve expensive computations. It would be advantageous if the electrostatic potential could be obtained reliably from a refinement with a spherical atom model using only two charge parameters per atom (p_v and κ). In the case of GABA, the spherical atom refinement gives a map (Fig. 2 d) that reproduces the main features of the map derived from the refinement with higher multipoles (Fig. 2 a), although it can be seen that the electronegative trough at O(2) is shallower (−0.16 versus −0.26e/Å) and the electropositive region is relatively contracted. These effects arise because of the fact that in the spherical atom refinement most of the atomic charges correspond to atoms that are more nearly neutral.

Nevertheless, the results from the spherical atom refinement for GABA are promising. They indicate that the experimental determination of the electrostatic potential may be possible for much larger molecules. It remains necessary to explore the limitations and to seek possible improvements in the model used for spherical atom refinements. Probably the most important consideration will be whether the necessary resolution in the diffraction data can be obtained. From our experience, the data should extend at least to $(\sin \theta)/\lambda = 0.8$ Å^{-1} or $d = 0.7$ Å. Also, as emphasized above, the contribution of the hydrogen atoms to the total potential is important. It will be necessary to develop a satisfactory procedure for determining the positional and thermal parameters for hydrogen when crystals suitable for neutron diffraction are not available.

This research was supported by grants GM-39513 and HL-20350 from the National Institutes of Health. We are grateful to Dr. R. Shiono for the computer plotting routine and to Mrs. M. J. Klinger for assistance in preparing the manuscript.

REFERENCES

Brooks, B. R., R. E. Bruccoleri, B. D. Olafson, D. J. States, S. Swaminathan, and M. Karplus. 1983. CHARMM: a program for macromolecular energy, minimization and dynamics calculations. *J. Comput. Chem.* 4:187–217.

Clementi, E. 1965. Tables of atomic functions. *IBM J. Res. Dev.* 9:2–6 (see supplement with 16 pages of tables).

Coppens, P., T. N. Guru Row, P. Leung, E. D. Stevens, P. J. Becker, and Y. W. Yang. 1979. Net atomic charges and molecular dipole moments from spherical atom X-ray refinements and the relation between atomic charge and shape. *Acta Crystallogr.* A35:63–72.

Craven, B. M. 1987. Studies of hydrogen atoms in organic molecules. *Trans. Am. Cryst. Assoc.* 23:71–81.

Craven, B. M., and H. P. Weber. 1983. Charge density in the crystal structure of γ-aminobutyric acid at 122K: an intramolecular methylene H bridge. *Acta Crystallogr.* B39:743–748.

Craven, B. M., H. P. Weber, X. M. He, and W. T. Klooster. 1993. The POP procedure: computer programs to derive electrostatic properties from Bragg reflections. Technical Report TR-93-1. Crystallography Department, University of Pittsburgh, Pittsburgh.

De Robertis, E. 1986. GABAergic neurotransmission. An overview. *In* GABA and Endocrine Function. G. Racagni, and A. O. Donoso, editors. Raven Press, New York. 1–12.

He, X. M., S. Swaminathan, B. M. Craven, and R. K. McMullan. 1988. Thermal vibrations and electrostatic properties of parabanic acid at 123K and 298K. *Acta Crystallogr.* B44:271–281.

Hehre, W. J., R. F. Stewart, and J. A. Pople. 1969. Self-consistent molecular-orbital methods. I. Use of Gaussian expansions of the Slater-type atomic orbitals. *J. Chem. Phys.* 51:2657–2664.

Hirshfeld, F. L. 1971. Difference densities by least-squares refinement: fumaric acid. *Acta Crystallogr.* B27:769–781.

Hösli, L., and E. Hösli 1983. Electrophysiological and autoradiographic studies on GABA and glutamate neurotransmission at the cellular level. *In* Glutamine, Glutamate and GABA in the Central Nervous System. L. Hertz, E. Kvamme, E. G. McGeer, and A. Schousboe, editors. Alan R. Liss, New York. 441–455.

Klooster, W. T., and B. M. Craven. 1992. The electrostatic potential for the phosphodiester group determined from X-ray diffraction. *Biopolymers.* 32:1141–1154.

Klooster, W. T., S. Swaminathan, R. Nanni, and B. M. Craven. 1992. Electrostatic properties of 1-methyluracil from diffraction data. *Acta Crystallogr.* B48:217–227.

Pearlman, D. A., and S. H. Kim. 1990. Atomic charges for DNA constituents derived from single-crystal X-ray diffraction data. *J. Mol. Biol.* 211:171–187.

Stewart, R. F. 1976. Electron population analysis with rigid pseudoatoms. *Acta Crystallogr.* A32:565–574.

Stewart, R. F. 1979. On the mapping of electrostatic properties from Bragg diffraction data. *Chem. Phys. Lett.* 65:335–342.

Stewart, R. F. 1982. Mapping electrostatic potentials from diffraction data. *God. Jugosl. Cent. Kristalogr.* 17:1–24.

Stewart, R. F. 1991. Electrostatic properties of molecules from diffraction data. *In* The Application of Charge Density Research to Chemistry and Drug Design. G. A. Jeffrey, and J. F. Piniella, editors. Plenum Publishing Corp., New York. 63–101.

Stewart, R. F., and M. A. Spackman. 1983. Valray users manual. Department of Chemistry, Carnegie Mellon University, Pittsburgh.

Su, Z., and P. Coppens. 1992. On the mapping of electrostatic properties from the multipole description of the charge density. *Acta Crystallogr.* A48:188–197.

Swaminathan, S., and B. M. Craven. 1984. Electrostatic properties of phosphorylethanolamine at 123K from crystal diffraction data. *Acta Crystallogr.* B40:511–518.

van der Wal, R. J., and R. F. Stewart. 1984. Shell population and κ refinements with canonical and density-localized scattering factors in canonical form. *Acta Crystallogr.* A40:587–593.

Watson, G.N. 1966. A Treatise on the Theory of Bessel Functions. 2nd ed. Cambridge University Press, London. 404.

Weber, H. P., and B. M. Craven. 1987. Structure and charge density of the 1:1 complex of thiourea with parabanic acid at 298K. *Acta Crystallogr.* B43:202–209.

Weber, H. P., B. M. Craven, and R. K. McMullan. 1983. The neutron structure of and thermal motion in γ-aminobutyric acid (GABA) at 122K. *Acta Crystallogr.* B39:360–366.

Weiner, S. J., P. A. Kollman, D. T. Nguyen, and D. A. Case. 1986. An all atom force field for simulations of proteins and nucleic acids. *J. Comput. Chem.* 7:230–252.